AIChE

Hysteresis in Cloud Heights During Solid Suspension in Stirred Tank Reactor: Experiments and CFD Simulations

Madhavi V. Sardeshpande
Industrial Flow Modeling Group, National Chemical Laboratory, Pune 411 008, India, and Dept. of Chemical Engineering, Indian Institute of Technology Bombay, Powai, Mumbai 400 079, India

Vinay A. Juvekar
Dept. of Chemical Engineering, Indian Institute of Technology Bombay, Powai, Mumbai 400 079, India

Vivek V. Ranade
Industrial Flow Modeling Group, National Chemical Laboratory, Pune 411 008, India

DOI 10.1002/aic.12191
Published online June 10, 2010 in Wiley Online Library (wileyonlinelibrary.com).

Solid suspension in stirred tank reactor is widely used in process industries for catalytic reactions, dissolution of solids, crystallization, and so on. Suspension quality is a key issue in design and operation of stirred reactor and its determination is not straight forward. Cloud height measurements of solid suspension provide a relatively simple way to quantify quality of suspension. In this work, experiments were carried out to quantify variation of cloud heights with impeller speed and particle characteristics. These measurements were carried out using visual observations, image analysis, and ultrasound velocity profiler techniques. The obtained data demonstrated the existence of hysteresis in cloud heights with respect to impeller speed. Apart from possible applications in reducing power required for achieving desired solid suspension quality, the existence of hysteresis also provides a new way to evaluate computational fluid dynamics (CFD) simulations of solid–liquid flows in stirred vessels. An attempt was made to capture observed hysteresis in cloud heights in CFD simulations. The simulated results were compared with the experimental data. The presented models and results (experimental and computational) will be useful for simulating complex solid–liquid flows in stirred reactors. © 2010 American Institute of Chemical Engineers *AIChE J,* 56: 2795–2804, 2010

Keywords: hysteresis in cloud height, solid velocity profiles, CFD

Introduction

Reliable design and scale-up of solid–liquid stirred reactors crucially depends on quality of solid suspension. Suspension quality in stirred tank reactor (STR) depends upon complex interactions of impeller generated flow, turbulence and particle characteristics (solid loading and particle size). Recent advances in computational fluid dynamics (CFD) and

Correspondence concerning this article should be addressed to V. V. Ranade at vv.ranade@tridiagonal.co.in.
Current Address of V.V. Ranade: Tridiagonal Solutions Pvt. Ltd., 100 NCL Innovation Park, Pune 411008, India.
V.V Ranade: On leave from National Chemical Laboratory, Pune 411 008, India.

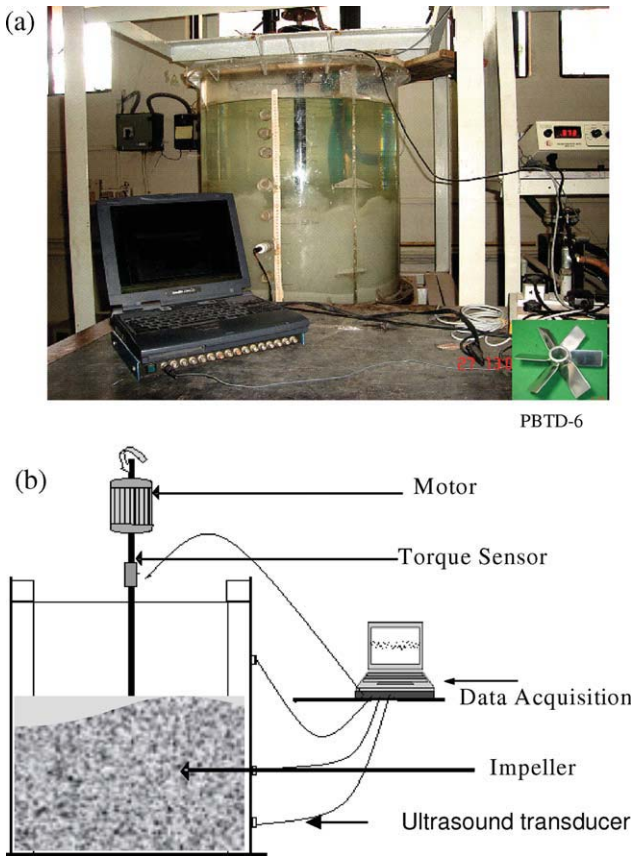

Figure 1. Experimental set up (a) pictorial view and (b) schematic view.

[Color figure can be viewed in the online issue, which is available at wileyonlinelibrary.com.]

experimental techniques provide new ways to characterize solid–liquid systems in STRs. Several attempts[1–3] of simulating solid–liquid stirred tanks using CFD have been made by previous researchers. However, many of these models were evaluated by comparing results for solid volume fraction profiles averaged over reactor cross section. Unfortunately, comparison of cross-sectionally averaged solid volume fraction is not an effective way to discriminate closure models of interphase drag force. Thus, there is still no consensus on closures of interphase drag force terms for solid–liquid suspension in these published studies. There are relatively few studies available related to measurements of local solid velocity profiles[4,5] and cloud height of suspended solids.[6–8]

In recent published studies,[9,10] flow hysteresis was observed that linked to flow stability in fuel cells. Flow hysteresis phenomenon indicated multiple flow distribution at same flow conditions but by varying ascending and descending way of operation. Similar methodology was carried out for the first time in solid–liquid stirred tank to achieve better solid distribution with minimum power using hysteresis phenomenon in cloud height.

In this study, possible use of cloud height measurements for better understanding of solid–liquid flow in stirred tanks and for critical evaluation of CFD models was explored. Experiments were conducted in an acrylic tank to visualize solid–liquid flow. During agitation of solid–liquid system, one can visually observe an interface that distinguishes two regions in the vessel: a region containing suspended solids (cloud region) and clear liquid region. At a particular impeller rotation, solids get lifted to maximum height within the fluid forming an interface between suspended solids and clear liquid. The height of this interface from tank bottom is called as the "cloud height." This interface (i.e., cloud height) depends on existing fluid and particle characteristics, vessel and impeller configuration, and impeller speed. Our preliminary visual observations of cloud height indicated that, if different paths followed in operating conditions such as increase of impeller speed from lower to higher rpm and vice versa then there is a possibility of "hysteresis" to occur in cloud height measurements. This information directed toward further experimental and computational investigations. Apart from possible applications in reducing power required for achieving desired solid suspension quality, existence of hysteresis may also provide a new way to evaluate CFD simulations of solid–liquid flows in stirred vessels. In this work, systematic experimental and computational investigations were carried out for cloud height variation with increasing and decreasing impeller speeds. Considering limitations of visual observation technique, observed hysteresis was confirmed by characterizing cloud heights using image analysis and ultrasound velocity profiler (UVP) technique.

Experimental Set Up and Measurement Techniques

Dimensions of experimental set up were decided up on standard geometrical configuration for pilot plant scale model. Experiments were carried out in a fully baffled, flat bottom cylindrical reactor ($T = 0.7$ m, H/T-1). Pictorial view and a schematic diagram of experimental setup are shown in Figures 1a, 1b. Four baffles of width T/10 were mounted diametrically opposite and perpendicular to the reactor wall. A shaft of an impeller ($d_s = 0.032$ m) was concentric with the axis of reactor. Down-pumping six-bladed Pitched Blade Turbine (PBTD-6-D_i-0.2 m) was used in this work. Impeller off-bottom clearance was (C-T/3) measured from mid of impeller blade height. The working fluid was tap water ($\rho_l = 1000$ kg/m^3) and solids as glass bead particles ($\rho_s = 2500$ kg/m^3) of diameter 50 and 250 μm were used. Preliminary cloud height measurements indicated that a clear discrimination of solid–liquid interface was possible in case of 250-μm-size particle for all operating conditions. However, in case of 50-μm-size particles, the appearance of the slurry was "milky," making it difficult to clearly recognize the solid–liquid interface. Therefore, this study was focused only on 250-μm-size particle rather than 50-μm-size particles. Experiments were carried out for four different solid loadings viz. 1, 3, 5, and 7 v/v % and 10 different impeller speeds ranging from 150 to 602 rpm. Cloud height and its hysteresis with impeller speed was measured visually. Image analysis and UVP technique were used to confirm the "hysteresis" observed in cloud height. Detailed discussion of these techniques is given in the following subsections.

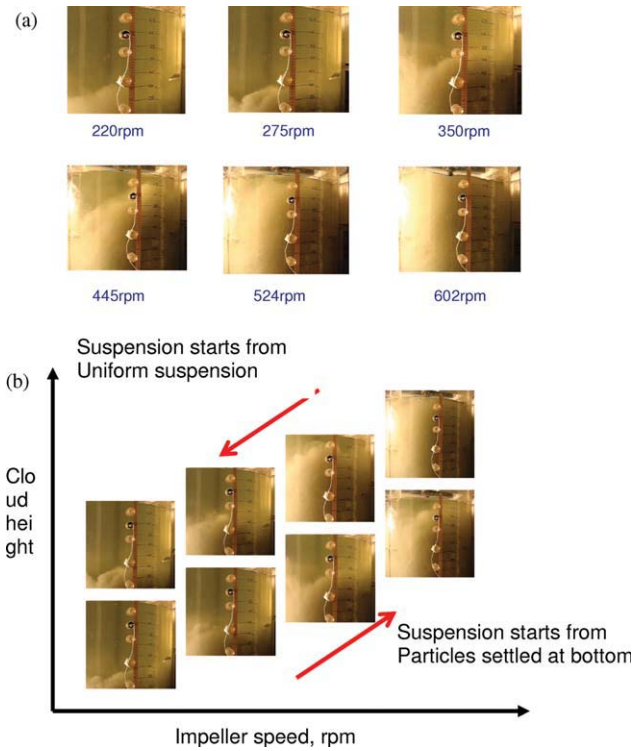

Figure 2. Visual observation study from side wall of the stirred tank at 7 v/v %, d_p: 250 μm.

(a) cloud height measurements for six different impeller-speeds and (b) two different operating approaches for hysteresis in cloud height. [Color figure can be viewed in the online issue, which is available at wileyonlinelibrary.com.]

Visual observation

Visual observation of cloud height measurements indicated that cloud height was not constant across the diameter of tank due to an inherently unsteady flow in solid–liquid stirred vessel. Typical photographs of cloud at various impeller speeds are shown in Figure 2a. At a fixed impeller speed, the range of cloud height variation (i.e., maximum and minimum) was noted down and arithmetic mean of upper and lower limits of this range was considered and reported as the mean cloud height. It was also observed that at all impeller speeds, average cloud height measured was unchanged after 10 min. Therefore, cloud height measurements were recorded with 10 min delay from the instance at which impeller speed was set. Cloud height measurements were carried out first with gradually increasing impeller speed from 150 to 602 rpm (i.e., up to attainment of uniform suspension) and then gradually decreasing from 602 to 150 rpm. A sample of photographs of such experiments are shown in Figure 2b.

Image analysis technique

Cannon Powershot A630 digital camera that couples 8.0-megapixel CCD imaging sensor with a 4× optical zoom lens (35 mm-equivalent focal range of 35–140 mm wide angle) was used to record videos during solid suspension. Black color cloth was used as a background and light (using halogen lamp) was focused into a tank from the top. Before starting the measurements of cloud height, calibration image was acquired for an exact height of a tank. With the camera set in fixed position (during calibration), videos were recorded at a speed of 30 fps for duration of 60 s. Captured videos were analyzed using image analysis software, that is, "Image ProPlus" (MediaCybernetics, USA), and frames from video files were extracted for image processing. As light source was focused from top, into a tank, maximum brightness was observed at upper part of cloud of particles compared to lower solid rich region and upper clear liquid region. Typical screenshot using the Image Pro-plus software is shown in Figure 3a. At any instantaneous snapshot, cloud height was never constant along the diameter due to liquid circulations. Therefore, light intensity profile along the reactor height was estimated at five different radial locations. The radial-average profile of these light intensity profiles was used for further analysis. The averaged light intensity was plotted against dimensionless tank height. Reproducibility of light intensity was verified by repeating all experiments for three times. Similar to visual observation technique, average light intensity (i.e., average between maximum and minimum intensity) near the top surface was marked. Transition from maximum to minimum intensity

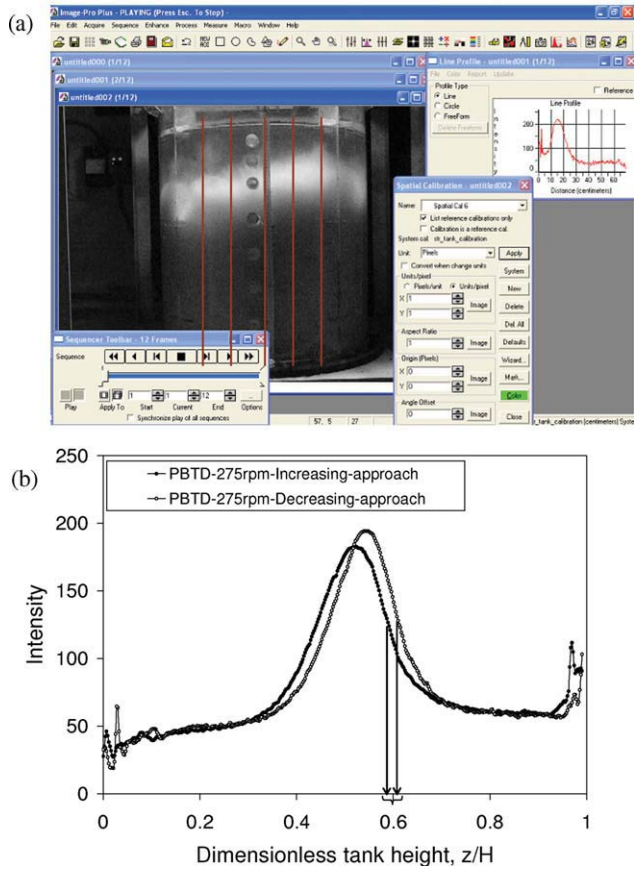

Figure 3. Hysteresis in cloud height confirmed using (a) Image analysis technique and (b) Intensity vs. dimensionless tank height.

[Color figure can be viewed in the online issue, which is available at wileyonlinelibrary.com.]

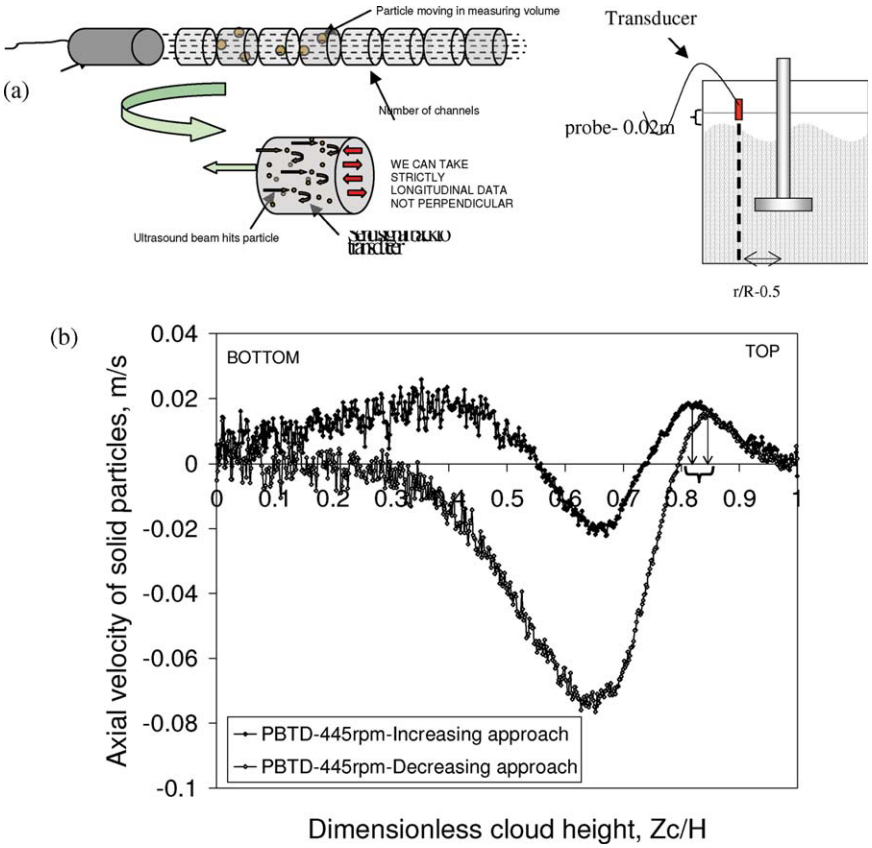

Figure 4. Hysteresis in cloud height confirmed using (a) Ultrasound Velocity Profiler technique, (b) Axial velocity Profile vs. dimensionless cloud height.

[Color figure can be viewed in the online issue, which is available at wileyonlinelibrary.com.]

near top surface directed toward dynamic solid–liquid interface with respect to every impeller speed. Therefore, an average intensity toward top surface was represented as "cloud height." Videos were recorded for increasing and decreasing impeller speeds (range of 150–602 rpm). It was also observed that for both increasing/decreasing approaches of impeller speeds showed quantitatively different cloud heights. This confirmed existence of hysteresis in cloud height (see Figure 3b).

UVP technique

The principle of the UVP technique is illustrated in Figure 4a. UVP transducer with an acquiring capacity of 1 MHz is used in this work. The transducer was set at an angle normal to the vessel wall and was allowed to transmit short emission of ultrasound along the transducer axis (i.e., measurement axis). Ultrasound pulse is transmitted in the measurement axis and hits the scattering particle and is echoed back which is received by the same transducer with a time delay. The delay in time and distance of particle from transducer are used to measure the particle velocity. The only requirement for UVP technique is that the fluid must contain sufficient amount of suspended particles on which scattering of ultrasound can be produced. For quantitative confirmation of hysteresis study, UVP transducer was inserted vertically into a tank (radial location between vessel wall and impeller i.e., $r/R = 0.5$) and 2 cm below the liquid surface so as to measure axial solid velocity profiles as shown in Figure 4b. Data were recorded for a period of 2400 s. Time averaged axial velocity profiles of solid particles were measured at increasing/decreasing impeller speed. Because of the weak circulation loop in the upper region, distinguishing axial velocity profile direction was observed and corresponding height was considered as "cloud height." The liquid below this height was solid-rich, whereas above it there was only an occasional visit by a few solids. A sample result of such the axial velocity profile is shown in Figure 4b at 445 rpm.

Computational Modeling

Geometrically, similar computational domain of stirred vessel was constructed with PBTD-6 for CFD simulations of solid–liquid flow as shown in Figure 5. Multiple reference frame approach was used to model the rotating impeller region in a rotating framework, while the surrounding region was solved in a stationary framework. Steady state simulations were carried out, wherein impeller–baffle interactions were accounted by a suitable coupling at an interface between the two regions. Two-phase flow (solid–liquid) is modeled using the Eulerian–Eulerian approach. In this approach, each phase is assumed to coexist at every point in each unit cell in the form of interpenetrating continua. It solves the continuity and momentum equations for each phase

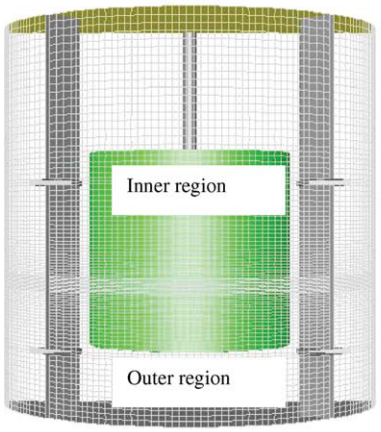

Grid details:		
T – 0.7 m	H/T – 1	Di – 0.2m
$r \times \theta \times z$	58 ×93 ×93	
Impeller	12 ×1 ×20	
Grid size	501642	

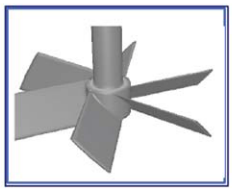

(a) PBTD - 6

Figure 5. Computational domain with PBTD-6.

[Color figure can be viewed in the online issue, which is available at wileyonlinelibrary.com.]

separately and coupled with each other through pressure and interphase exchange coefficients. Many applications involving solid–liquid flows in STR are in the turbulent regime. Therefore, Reynolds averaged mass and momentum balance equations were solved for each phase in this work.

The continuity equation and momentum balances for the liquid–solid phases were used as per Fluent manual for study of solid hold up profiles inside the vessel. $\vec{F}_{12,i}$ is the time-averaged interphase drag force in i direction and $\alpha_q \rho_q g_i$ is the external body force on liquid phase. The term p_s represent solid pressure that accounts for the force due to particle interactions. This term has been modeled according to the Kinetic Theory of Granular Flows.[11] The contribution of the turbulent dispersion, F_{DF}, is likely to be significant as previously reported numerical studies.[12–15] They highlighted the importance of modeling of turbulent dispersion force while simulating solid suspension in stirred reactor. It should be noted that the contribution of turbulent dispersion force is significant only when the size of the turbulent eddies are larger than the particle size. In the case of solid–liquid stirred reactor, even for laboratory scale, the ratio of the largest energy containing eddy (in mm) and the particle size was found to be around 10. Thus, the turbulent dispersion force (F_{DF}) was modeled in terms of turbulent diffusivity term, D, and included into momentum equation (see Fluent USA, manual).

The standard k-ε turbulence model with mixture properties was used. Standard values of the k-ε model parameters have been used in the present simulations ($C_1 = 1.44$, $C_2 = 1.92$, $C_\omega = 0.09$, $\sigma_k = 1.0$ and $\sigma_\varepsilon = 1.3$). The standard k-ε turbulence model with mixture properties was used as reported by Montante and Magelli[16]; the mixture model leads to similar results obtained using the standard k-ε model for each phase and also requires significantly lower computation time.

Interphase Exchange Term

The interphase momentum exchange terms make the two-phase flow simulations fundamentally different from the simulation of single-phase flows. The interphase momentum exchange term consist of four different forces: Basset history force, lift force, virtual mass force, and drag force discussed by Ranade.[17] The influence of these forces on the simulated solid holdup profile was studied by Ljungqvist and Rasmuson.[12] They have found very little influence of the virtual mass and lift force on the simulated solid holdup profiles. Considering this, in this work, these forces were neglected and only drag force was considered. The drag force termed as

$$F_{12,i} = -\frac{3\alpha_1\alpha_2\rho_1 C_D\left(\sum(U_{2,i}-U_{1,i})^2\right)^{0.5}(U_{2,i}-U_{1,i})}{4d_p} \quad (1)$$

where

$$\frac{C_D - C_{D_o}}{C_{D_o}} = K \times \left(\frac{d_p}{\lambda}\right)^3 \quad (2)$$

Estimation of drag is critical for accurate prediction of solid concentration distribution (suspension quality). In solid–liquid stirred reactor, interphase exchange coefficient C_D, is a complex function of drag coefficient in stagnant liquid (C_{Do}), solid hold up and smallest eddy length scale, that is, Kolmogorov length scale. This length scale depends on turbulent dissipation rate and plays significant role in solid suspension. Different drag correlations[18,19] have been used for the prediction of solid concentration distribution in stirred vessels (some of which are listed in Table 1). Predicted results of the CFD model based on drag correlations proposed by Brucato et al.[20] and Khopkar et al.[3] were compared with the experimental data of Yamazaki[21] and GodFrey and Zhu.[22] It was found out that modified Brucato's correlation[3] was more suitable for the prediction of the local solid hold up than Brucato's correlation.[20] The main focus of this work was to extend and evaluate the CFD models by using these to capture hysteresis in cloud height in stirred vessels.

Numerical Solution

Computational model is solved using a commercial CFD solver Fluent 6.3.26 (ANSYS, USA). The grid generation

Table 1. Various Drag Correlations for Solid–Liquid System

Author	Proposed Drag Correlation	Remarks
Schiller and Naumann (1933)[18]	$C_D = \frac{24}{Re_P}(1 + 0.15{Re_P}^{0.687})$	Developed for single particle settling in stagnant fluid
Magelli et al. (1990)[19]	$\frac{U_s}{U_t} = 0.4\tan h\left(\frac{16\lambda}{d_p} - 1\right) + 0.6$	Measured settling velocity of particle turbulent fluid and proposed correlation for slip velocity
Brucato (1998)[20]	$\frac{C_D - C_{D0}}{C_{D0}} = 8.76 * 10^{-4}\left(\frac{d_p}{\lambda}\right)^3$	Developed for Taylor-Coutte type apparatus
Kopkar et al. (2006)[3]	$\frac{C_D - C_{D0}}{C_{D0}} = 8.76 * 10^{-5}\left(\frac{d_p}{\lambda}\right)^3$	Developed for solid–liquid system in stirred tank

tool, GAMBIT 2.3.16 was used to generate the computational domain. The predictions of flow characteristics, especially turbulence quantities are sensitive to the grid distribution within the solution domain and discretization scheme. Geometry was modeled using three different grid size distributions to check grid independency with total number of computational cells (hexahedral cells) as 302045, 501746, and 839573. QUICK (Quadratic Upstream Interpolation for Convective Kinetics) discretization scheme was used in all these simulations. It was observed that for single phase using 501746 cell count predicted reasonable well in agreement power number and also remained constant even after further refinement of grid. As a result of this, presented numerical simulations in this article were carried out with grid cells of 501746 ($r \times \theta \times z$: 58 × 93 × 93).

Results and Discussion

In this section, the quantification of cloud height measurements for various particles size, impeller speed, and solid loading is briefly discussed. The hysteresis observed in cloud height measurements for the varying impeller speed is presented along with the simulation results.

Influence of impeller speed and solid loading on cloud heights

Impeller speed and solid loading are interlinked parameters and play a vital role in determining prevailing cloud height in stirred vessels. Here, cloud height measurements were done for 1 to 7 v/v % solid loading at various impeller speeds. The measured variation of cloud height with impeller speed at different solid loading is shown in Figure 6. It can be seen that for low solid leading of 1 v/v %, even the lowest impeller speed was adequate to suspend most of the solids. The cloud height was more than 90% even for the lowest impeller speed. Further increase in impeller speed, therefore, did not show any significant change. For higher solid loadings, interestingly, nonmonotonic behavior of cloud height with impeller speed was observed. When impeller speed was increased from 150 rpm, the observed cloud height decreased up to a certain impeller speed. Increase in impeller speed beyond this specific value resulted in increase in cloud heights. Similar nonmonotonic behavior of cloud height with respect to impeller speed was also observed by Takenaka et al.[8] The nonmonotonic behavior may be explained by observations of settled solid bed and prevailing flow patterns in the vessels.

At 3 v/v % solid loading and impeller speed of 150 rpm, it was observed that large amount of solid particles were settled at the vessel bottom. Only small fraction of solids particles were suspended in the liquid. The effective suspended solid loading was, therefore, quite low, and solids were suspended up to higher levels resulting in higher cloud height (high axial gradient in solid hold up). When impeller speed increased to 220 rpm, flow stream from impeller impinges on the settled solid bed leading to suspension of more solid particles. This resulted into suspension of higher solid volume fraction from bottom of vessel affecting effective slurry density and flow near impeller. This resulted into lower cloud height than that observed at 150 rpm. At 150 rpm, average fluid circulation velocity was 0.043 U_tip. However, at 220 rpm, the average fluid circulation velocity was found to be 0.021 U_tip (thus even in absolute terms, average velocity was lower than that for 150 rpm). With further increase in impeller speed beyond 220 rpm, the bed region below the impeller which reduces the strength of impeller flow stream vanishes and leads to unrestricted flow (circulation velocity increases, that is, 0.021 U_tip to 0.085 U_tip) resulting into higher cloud heights. At 445 rpm, most of solids were more or less uniformly suspended and, therefore, further increase in impeller speed does not affect the cloud height. With this background, hysteresis in cloud height was studied for two different solid loadings are discussed in the following section.

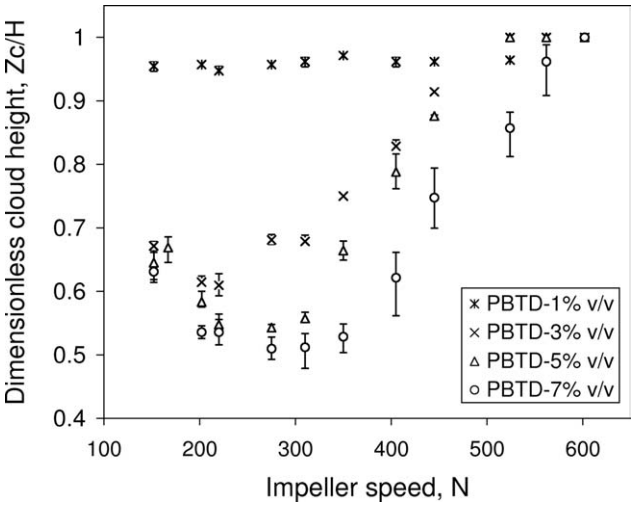

Figure 6. Effect of Re on cloud height at different solid loading, PBTD-6.

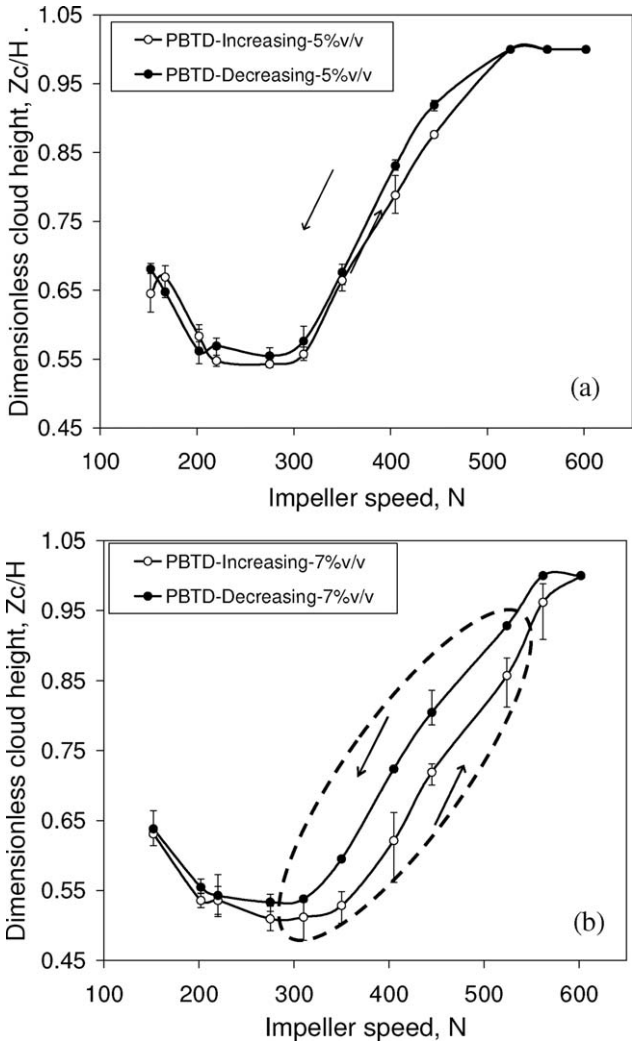

Figure 7. Effect of solid loading on hysteresis in cloud height with visual observation.

(a) $\varepsilon_s = 5$ v/v % (b) $\varepsilon_s = 7$ v/v %.

Hysteresis in cloud height measurements

Experiments were carried out to study hysteresis in cloud height measurements for different solid loadings (1–7 v/v %). It was observed that hysteresis in cloud height was not remarkably noticed for solid loading lower than 5 v/v % solid loading. The hysteresis was observed for 5 v/v % solid loading and was prominent at 7 v/v % solid loading, as shown in Figures 7a, 7b. The observed differences in cloud heights may appear to be due to unsteady nature of solids suspension. To ensure that the observed hysteresis is not due to transient effects, experiments were carried out for these two solid loading for a substantial time. The time history of cloud height measurements are shown in Figure 8a. It was observed that with change in operating conditions there was difference in cloud heights for same impeller speed even after 30 min. The hysteresis was also confirmed (discussed in the second section) using image analysis and UVP techniques for 7 v/v % solid loading at impeller speeds 220, 275, 350, and 445 rpm as shown in Figure 8b. Observed hysteresis by all three mentioned experimental techniques were within the range of $\pm 10\%$ confirming the existence of hysteresis in cloud height for solid–liquid STRs.

It is interesting to note that hysteresis is prominent at intermediate impeller speeds. For example, at 7 v/v % solid loading, hysteresis was prominent between 220 to 445 rpm impeller speeds. At low impeller speeds, cloud height is quite small and the hysteresis is not noticeable. At very high impeller speeds (closer to uniform suspension speed), the liquid velocities in the vessel are significant which can lift almost all the solids from the bottom surface. The magnitude of hysteresis is, therefore, quite small under these conditions as well. At intermediate impeller speeds, the liquid velocities are not strong enough to completely suspend settled bed from the bottom surface. In such a case, there is a significant difference in cloud heights when started from completely settled bed and from uniformly suspension. This is why larger magnitudes of hysteresis occur at intermediate impeller speeds. In light of this, further studies of hysteresis using

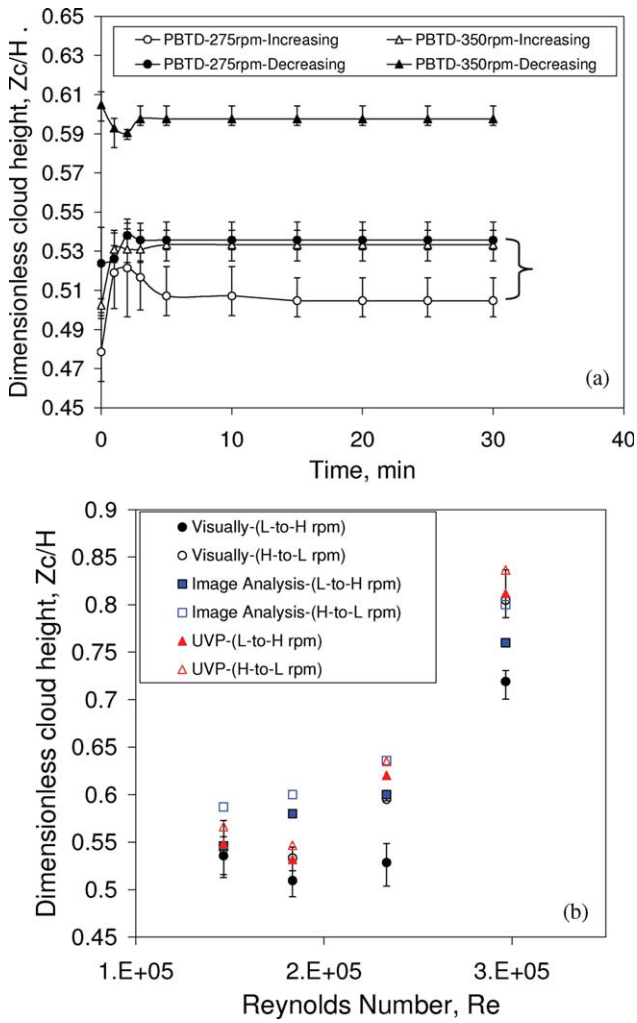

Figure 8. Confirmation of hysteresis study at 7 v/v % solid loading.

(a) Cloud height behavior at different time scale and (b) observed hysteresis confirmed with all three techniques. [Color figure can be viewed in the online issue, which is available at wileyonlinelibrary.com.]

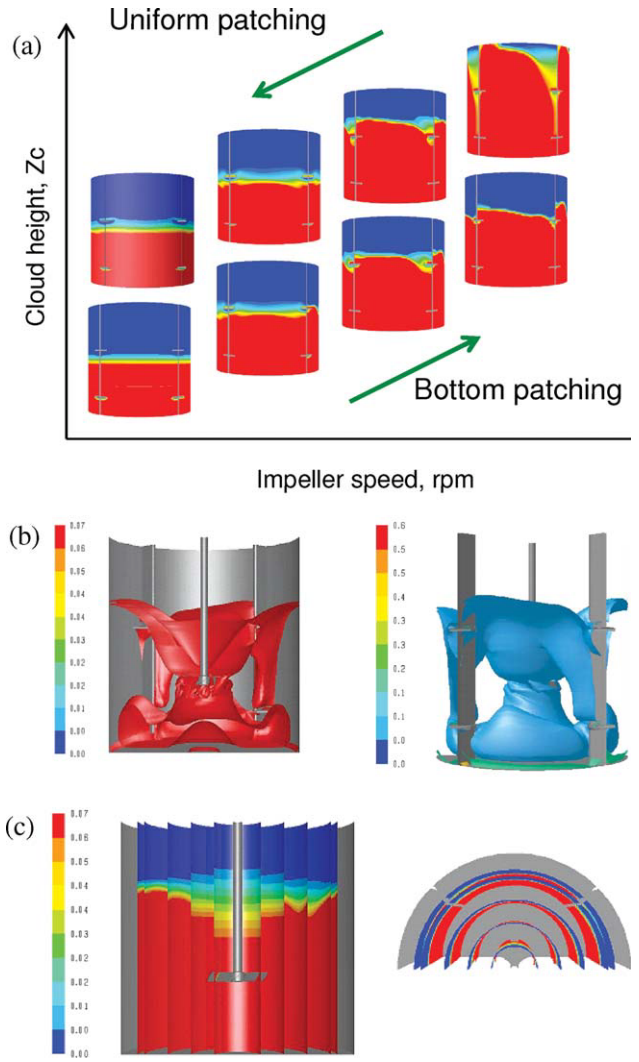

Figure 9. (a) Two initialization approaches for hysteresis study (blue:0 and red:0.07), (b) Nonuniform concentration distribution of solids observed, and (c) Front view as well as top view of radial planes from impeller to wall.

[Color figure can be viewed in the online issue, which is available at wileyonlinelibrary.com.]

CFD simulations were carried out for these conditions which are discussed in the following.

Hysteresis in cloud height by CFD simulations

The observed hysteresis of cloud heights in stirred vessels is mainly because of the different effective drag experienced by solid particles based on the current state of solid suspension. Natural choice of the simulations could be full unsteady simulations. However, such full unsteady simulations require order of magnitude larger computing resources and turn around time. In this work, therefore, we have carried out steady state simulations. The different initial conditions were, therefore, represented by different initial guess/conditions. Two different initial conditions were used to capture the observed hysteresis in cloud height in CFD simulations. In the first case: the initial condition (guess) of solid volume fraction was set such as to mimic the settled bed of solids at the tank bottom (to capture cloud height in increasing order of impeller speed). In the second case: the initial condition (guess) of uniform solid volume fraction (i.e., $\varepsilon_s = 0.07$) through out the tank was used (to capture cloud height in decreasing order of impeller speed). Steady state simulations were carried out with both the cases using Brucato's[20] and Khopkar et al.[3] drag correlations. The latter correlation was shown to predict experimental data of Yamazaki[21] and GodFrey and Zhu[22] reasonably well.

The predicted contour plots of solid volume fractions using two different initial conditions and Brucato's[20] drag correlation are shown in Figure 9a. Brucato's correlation[20] consists of Kolmogorov length scale (i.e., function of rate of turbulent dissipation). In both the approaches, initially the turbulent dissipation rate was considered equal to converged single phase simulated values. As simulation proceeds, this turbulent dissipation rate value was changed. After every 500 iterations, the modified value of volume averaged turbulent dissipation rate was used to recalculate Kolmogorov length scale and modify the value of existing drag coefficient using the developed UDF (user defined function). This procedure of adjusting drag coefficient was followed for both the cases. The converged results for these two cases showed marked differences in the converged values of the turbulent dissipation rate and, therefore, in effective interphase drag and cloud heights. The approach used in this work was, therefore, able to capture hysteresis in cloud heights. It was also encouraging to observe "funneling" kind of solid distribution, solids being drawn toward the impeller and also nonuniformity of the cloud height across the tank diameter as observed in the experiments (Figure 9b). The "funneling" of solids explained the different axial and radial levels, that is, uneven solid distribution inside the vessel. Therefore, an attempt was made here to adopt circumferential axial averages of solid volume fraction at five different radial locations as shown in Figure 9c. These different levels of solid volume fractions at five radial locations were used for quantifying the cloud height as

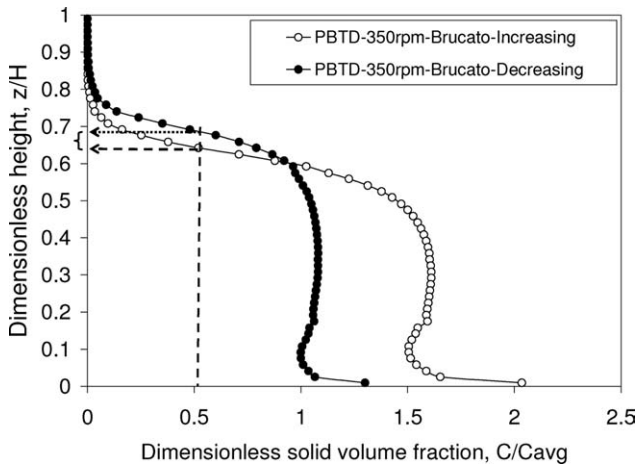

Figure 10. Difference in cloud height with two approaches at 350 rpm, 7 v/v %.

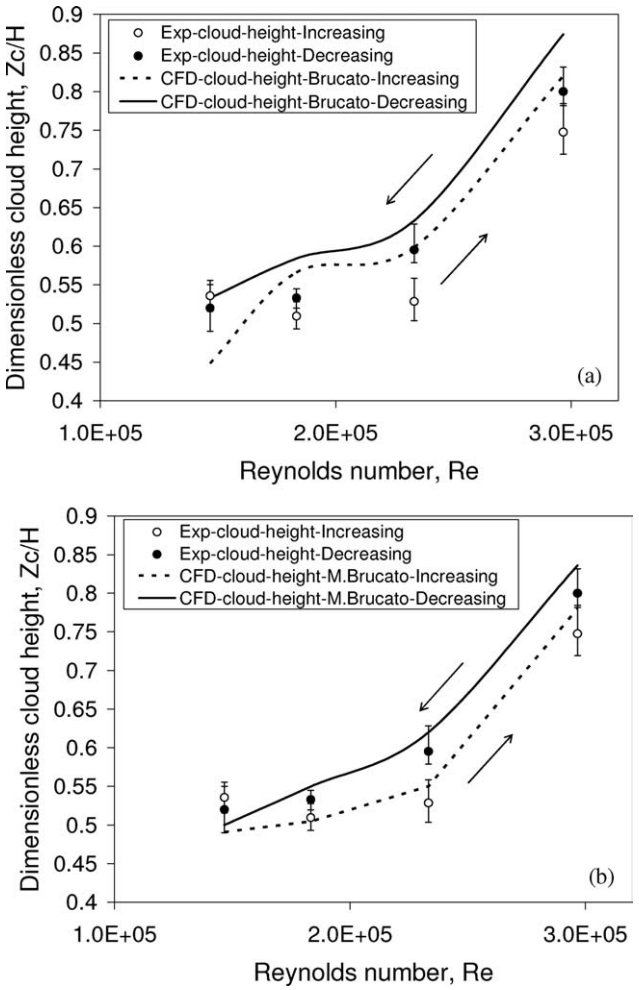

Figure 11. Hysteresis in cloud height using two different drag correlations.

(a) Brucato's drag correlation and (b) modified Brucato's drag correlation

shown in Figure 10. From the plot of z/H vs. C/C_{avg} and visually observed experimental values, a criterion was decided for estimating cloud height from the CFD simulations. It was found that if C/C_{avg} of CFD simulations equals to 0.5 then corresponding height agreed with the experimental cloud height and was, therefore, used to quantify cloud height from CFD (see Figure 10).

Similar course of action was followed for further simulations using modified Brucato's correlation, that is, of Khopkar et al. [3] These results indicated that the drag correlation of Brucato et al. [20] over predicted hysteresis in cloud height. The results predicted with the drag correlation of Khopkar et al [3] were found to be closer to the experimental data (i.e., with visual technique) of hysteresis in cloud height (see Figures 11a, 11b). Thus, the CFD models with appropriate initial guess were found to capture observed hysteresis in cloud heights with respect to impeller speed. The observed hysteresis may be used to evolve operating protocols to ensure better solids suspension without increasing time averaged power requirements.

Conclusions

Suspension of solid particles in solid–liquid stirred vessel was experimentally and computationally studied for solid loading upto 7 v/v %. Hysteresis in cloud height of suspended solids with respect to impeller speed was observed. The observed hysteresis was also captured in the CFD models. The key conclusions based on this work are listed below:

(a) Cloud height varies nonmonotonically with impeller speed especially at higher solid loading.

(b) Cloud height exhibits hysteresis with respect to impeller speed and follows different routes with increasing and decreasing impeller speed. The hysteresis in cloud height increases with solids loading and was quite prominent at 7 v/v % solid loading.

(c) CFD models with appropriate initial guess and drag correlations capture the observed hysteresis in cloud heights.

(d) The reported results provide a useful way to evaluate different drag correlations for simulating solid–liquid suspension in stirred vessels.

Notation

C = impeller off-bottom clearance, m
C_D = drag coefficient in turbulent liquid
C_{Do} = drag coefficient in still liquid
C/C_{avg} = Dimensionless solid distribution along height
D_i = impeller diameter, m
D_{12} = turbulent diffusivity, m/s
d_p = particle diameter, m
$\vec{F}_{12,i}$ = interphase drag force, N/m
F_{DF} = turbulent dispersion force
H = tank height, m
p_l = liquid pressure, N/m^2
p_s = solid pressure, N/m^2
T = Tank diameter, m
U_s = terminal settling velocity in still fluid, m/s
U_t = terminal settling velocity in turbulent fluid, m/s
g = acceleration due to gravity, m/s
z = axial coordinate, m

Greek letters

α = Volume fraction
ε = turbulent dissipation rate, m^2/s^3
λ = Kolmogorov length scale, m
ρ = density, kg/m^3
μ = viscosity, kg/(ms)
τ = shear stress, N/m

Subscripts

1 = liquid
2 = solid
q = phase number
t = turbulent

Literature Cited

1. Gosman AD, Lekakou C, Politis S, Issa RI, Looney MK. Multidimensional modeling of turbulent two-phase flows in stirred reactors. *AIChE J*. 1992;38:1946–1956.
2. Micale G, Montante G, Grisafi F, Brucato A, Godfrey J. CFD simulation of particle distribution in stirred reactors. *Trans IChemE*. 2000;78:435–444.
3. Khopkar AR, Kasat GR, Pandit AB, Ranade VV. Computational fluid dynamics simulation of the solid suspension in stirred slurry reactor. *Ind Chem Res Des*. 2006;45:4416–4428.

4. Guiraud P, Costes J, Bertrand J. Local measurements of fluid and particle velocities in stirred suspension. *Chem Eng J*. 1997;68:75–86.
5. Fishwick RP, Winterbottom JM, Stitt EH. Explaining mass transfer observations in multiphase stirred reactors: particle-liquid slip velocity measurements using PEPT'. *Catal Today*. 2003;79/80:195–202.
6. Hicks MT, Mayers KJ, Bakker A. Cloud height in solid suspension agitation. *Chem Eng Commun*. 1997;160:137–155.
7. Bujalski W, Takenaka K, Paolini S, Jahoda M, Paglianti A, Takahashi K, Nienow AW, Etchells AW. Suspension and liquid homogenization in high solids concentration stirred chemical reactors. *Trans Ichem E*. 1999;77:241–247.
8. Takenaka K, Takashi K, Bujalski W, Nienow AW, Paolini S, Pagaltini A, Etchells A. Mixing time for different diameters of impeller at a high solid concentration in an agitated vessel. *J Chem Eng Japan*. 2005;38:309–315.
9. Zhang LF, Bi HT, Wilkinson DP, Stumper J, Wang H. Gas-liquid two-phase flow patterns in parallel channels for fuel cells. *J Power Sources*. 2008;183:643–650.
10. Zhang LF, Du W, Bi HT, Wilkinson DP, Stumper J, Wang H. Gas-liquid two-phase flow distributions in parallel channels for fuel cells. *J Power Sources*. 2009;189:1023–1031.
11. Gidaspow D. Multiphase Flow and Fluidization: Continuum and Kinetic Theory Description. Boston, MA: Academic Press Inc, 1993.
12. Ljungqvist M, Rasmuson A. Numerical simulation of the two-phase flow in an axially stirred reactor. *Trans IChem E*. 2001;79:533–546.
13. Angst R, Harnack E, Singh M, Kraume M. Grid and model dependency of the solid/liquid two-phase flow CFD simulation of stirred reactors. Proceedings of the 11th European Conference of Mixing, Bamberg, Germany, October 14–17, 2003, 347–350.
14. Barrue H, Bertrand J, Cristol B, Xuereb C. Eulerian simulation of dense solid-liquid suspension in multi-stage stirred reactor. *J Chem Eng Jpn*. 2001;34:585–589.
15. Shirolkar JS, Coimbra CFM, McQuay MQ. Fundamental aspects of modeling turbulent particle dispersion in dilute flows. *Prog Energy Comb Sci*. 1996;22:363–378.
16. Montante G, Magelli F. Modeling of solids distribution in stirred tanks: analysis of simulation strategies and comparison with experimental data. *Int J Comput Fluid Dyn*. 2005;19:253–262.
17. Ranade VV. *Computational Flow Modelling for Chemical Reactor Engineering*. New York: Academic Press, 2002.
18. Schiller L, Neumann A. Uber die grundlegenden berechungen bei der schwer kraftaufbereitung. *Ver Dtsch Ingenieure*. 1933;77:318–320.
19. Magelli F, Fajner D, Nocentini M, Pasquali G. Solid distribution in reactors stirred with multiple impellers. *Chem Eng Sci*. 1990;45:615–625.
20. Brucato A, Grisafi F, Montante G. Particle drag coefficients in turbulent fluids. *Chem Eng Sci*. 1998;53:3295–3314.
21. Yamazaki H, Tojo K, Miyanami K. Concentration profiles of solids suspension in a stirred tank. *Powder Technol*. 1986;48:205–216.
22. Godfrey JC, Zhu ZM. Measurement of particle liquid profiles in agitated tanks. *AIChE Symp Ser*. 1994;299:181–185.

Manuscript received July 12, 2009, revision received Nov. 11, 2009, and final revision received Jan. 19, 2010.